Mathematical Biosciences and Engineering

MBE, 20(6): 9965–9991.
DOI: 10.3934/mbe.2023437
Received: 20 December 2022
Revised: 08 March 2023
Accepted: 16 March 2023
Published: 27 March 2023

http://www.aimspress.com/journal/MBE

Research article

Sulfate ions diffusion in concrete under coupled effect of compression load and dry-wet circulation

Jian Cao*, Tao Liu, Ziyang Han and Bin Tu

School of Civil and Architecture Engineering, Nanchang Institute of Technology, Nanchang 330099, China

*** Correspondence:** Email: caojian1980@126.com; Tel: 13879160967; Fax: (86) 79182096401.

Abstract: The diffusion of Sulfate ions in concrete is a complex process and affects the performance of concrete. Experiments on the time-dependent distribution of sulfate ions in concrete under the coupling of pressure load, dry-wet circulation, and sulfate attack, and the diffusion coefficient of sulfate ions with various parameters was tested. The applicability of the cellular automata (CA) theory to simulate the diffusion of sulfate ions was discussed. In this paper, a multiparameter cellular automata (MPCA) model was developed to simulate the impacts of load, immersion ways, and sulfate solution concentration for the diffusion of sulfate ions in concrete. The MPCA model was compared with experimental data, considering compressive stress, sulfate solution concentration, and other parameters. The numerical simulations verify the calculation results based on the MPCA model are in good agreement with the test data. Finally, the applicability of the established MPCA model was also discussed.

Keywords: cellular automaton; dry-wet circulation; sulfate ion; compression load; diffusion

1. Introduction

Sulfate erosion in concrete is a complex process combining physics, chemistry, and mechanics, with numerous influencing factors and severe consequences, and it is an important issue of the concrete durability. When concrete is eroded, the pores are filled with salt crystals, causing micropores to crack, which leads to ultimate bearing capacity of concrete decreased with age [1]. In actual engineering, concrete is subject to the dual effects of sulfate and load [2]. There is a consensus

among the research results that the deterioration of concrete will be accelerated by the coupling effect of load and environmental factors [3]. The combined effect will be more serious than the sum of individual effect.

Recently，many researchers have paid attention to the influence of sulfate attack on concrete, including mechanics [4], deformation [5] and durability [6]. The study of ion diffusion can increase our understanding of the distribution law of ion diffusion in concrete and provide a basis for the analysis of concrete damage. A chemical-mechanical model was firstly established by Tixier and Mobasher [7] to simulate the damage of concrete subjected to external sulfate erosion, Fick's second law was used to simulate sulfate ions diffusion, and the calculated values were also compared with the test data [8]. Bary [9] used a mixed-hybrid finite element (MHFE) method to get the sulfate ion concentration by continuous iteration. In simulating the diffusion of sulfate ions, Sarkar et al. [10] considered the concentration gradient and the chemical activity gradient. A diffusion model was proposed sulfate ion by Sun et al. [11], based on Fick's second law, concrete damage was considered on the basis of experiments. Ikumi et al. [12] proposed a simplified reaction transport equation of sulfate ions and used nonlinear numerical regression method to derive the most suitable parameters. The influence of interfacial transition zone on the diffusion of sulfate ions was explored by Sun et al. [13]. Chen et al. [14] studied the diffusion of sulfate ions in the coupling environment of chloride and sulfate. A strength degradation model of concrete which considers the corrosion depth under sulfate attack was established by Zhou et al. [15]. Liu et al. [16] analyzed the relationship between the sulfate solution concentration on the physical properties of concrete and found the load–displacement curves firstly increased and then decreased with the increase of solution concentration. Tang et al. [17] found that the coupling effect of load and sulfate had a great influence on the durability of concrete.

In the marine environment, the concrete structure can be divided into four zones, which are submerge, tidal, splash and atmospheric zones [18]. In these zones, dry-wet cycles often occur, which will accelerate the coupling of loading and sulfate, forming more complex effects [19]. At present, there is little research on this aspect. A numerical model was proposed to simulate the diffusion of sulfate ions under sulfate attack and dry-wet cycles by Li et al. [20], and the damage of concrete was taken into account. Tumidajski et al. [21] found the relationship between erosion time and sulfate ions diffusion coefficient in concrete based on Fick's second law. Gospodinov [22] presented the expression of effective diffusion coefficient of sulfate ions in concrete by using Fick diffusion law, the porosity in concrete and the numbers of sulfate ions participating in chemical reaction were taken as parameters. Yin et al. [23] developed a diffusion-reaction model subjected to the coupled axial loading and sulfate erosion. A two-dimensional model was established to study the diffusion of sulfate ions in concrete under the combination of loading and sulfate attack, in which stress and the sulfate ions concentration were accounted for [24].

CA was originally presented by Von Neumann [25]. CA is discrete in both space and time [26]. In recent years, CA has been widely used in different fields, which is regarded as an effective method for analyzing complex systems [27–31]. Biondini [32] firstly presented and applied CA to concrete structural systems for the diffusion process of ions, proposed the rule of evolution in d dimensions (d = 1, 2, 3), time-variant stress-dependent diffusivity and stochastic effects in the diffusion process were also considered [33]. The lifetime of concrete structures was also evaluated [34]. Most of the cellular automata equations used in concrete were developed by Biondini [35]. One of the advantages of CA is that its stochastic effects can better simulate the diffusion of ions [36–38].

Chloride diffusion was also very important for concrete, so researchers also used CA to explore the impact of different factors on chloride diffusion, such as chloride concentration, erosion time [39], and erosion depth [40]. The seismic performance of concrete constructs will change after being corroded, through the CA model to simulate diffusion of ions, the seismic performance of low-rise precast buildings [41], multistory precast concrete frames [42] and concrete bridges [43] subjected to corrosion were explored. The accuracy of CA models with different dimensions is different, the two-dimensional CA model could be more accurate for explaining the time-variant corrosion damage of concrete [44]. An improved approach with CA was presented by Ruan et al. [45] based on the mesoscopic features. According to the mechanism of chloride ion diffusion in concrete, a three-dimensional CA model for describing the diffusion process of chloride was proposed by Ma et al. [46].

This paper discusses the applicability of the CA model to model the diffusion behavior of sulfate ions. Then, experimental research was carried out on the time-dependent distribution of sulfate ions in concrete under the combined action of loading, dry-wet cycle, and sulfate erosion. The sulfate ions diffusion coefficient was investigated under various parameters. Additionally, considering the compressive stress level, the concentration of sulfate solution, and other factors, following the evolution rules [33] to adjust the evolutionary coefficients of the CA, a MPCA model was proposed. Under complex environmental conditions, it is challenging and creative to establish MPCA containing multiple parameters with physical significance. The main novelty of the approach proposed in this paper is the calibration of the dependency of the diffusivity coefficient on the stress level and other influencing variables. The parameters with physical meaning in the MPCA model make the model more practical and can play a better role in the actual engineering. The model simulates the sulfate ion diffusion process under the coupling of dry-wet circulation and load, the computation results on the basis of the MPCA model are in good agreement with experimental data. Finally, the applicability of the MPCA model was discussed.

2. Experimental procedure

2.1. Materials

Portland Cement (PC) of P.O 42.5, fine aggregates with fineness modulus of 2.6, crushed stone with grains size of 5–25 mm was used. The chemical compositions, physical and mechanical properties of cement were listed in Tables 1 and 2. The used fly ash was classified as Class II. The used slag was classified as S95. The water reducer used in this investigation was a QY-5 superplasticizer. The concrete mix proportion was listed in Table 3. Besides, the anhydrous sodium sulfate was purchased from Nanfeng Chemical Co. Ltd.

Table 1. Chemical composition of cement (/% by mass).

SiO_2	Al_2O_3	Fe_2O_3	CaO	MgO	SO_3	LOSS
22.14	5.65	4.77	64.21	0.94	1.02	0.82

Table 2. Physical and mechanical properties of cement.

Fineness (%) 80μm Sieve residue	Water requirement for standard consistency /%	Stability	Condensation time (min)		Flexural strength (MPa)		Compressive strength (MPa)	
			Initial setting	Final setting	3d	28d	3d	28d
2.9	28.3	qualified	92	200	5.8	9.5	29.1	60.6

Table 3. Mixing proportions of concrete (kg/m^3).

Cement	Fine aggregate	Coarse aggregate	Water	Fly ash	slag	Admixture
296	729	1050	172	81	63	8.80

Because the strength of the concrete mixed with fly ash still increased after 28 days curing [47]. The 28 days cube compressive strength, 90 days cube compressive strength, 90 days prism compressive strength, and 90 days elastic modulus of concrete specimens were tested, as listed in Table 4.

Table 4. Physical properties of concretes.

28d Cube compressive strength (MPa)	90d Cube compressive strength (MPa)	90d Compressive strength of prism (MPa)	90d Elastic Modulus (GPa)
54.30	66.62	50.45	45.26

In order to weaken the effect of the strength increase on the test results, this paper took the concrete specimens with 90 days curing.

2.2. Experimental parameters

The factors that affect the long-term performance of concrete can be divided into internal factors and external factors. The external factors include the different environments and load conditions, such as stress level, erosion solution concentration, and immersion method. The experiments were based on the coupling of load and erosion environment. The influence of external factors was mainly considered. The test factors considered in this study include load stress level (0, 15 and 30%), sulfate solution concentration (1, 5 and 10%), immersion ways: long-term immersion (LM) and dry-wet cycle (DW), erosion age (90, 180, 360 and 540days), as shown in Table 5. Therefore, the total number of specimens required for this test is shown in Table 6.

Table 5. Levels of the factors of the experiment.

Experimental factors	Parameter level
Compressive stress level (%)	0/15/30
Sulfate solution concentration (%)	1/5/10
Immersion ways	long-term immersion, dry-wet cycle
Erosion age (days)	90/180/360/540

Table 6. Quantity of the specimen.

Test content	Condition	Experimental factors	Total groups
Distribution of sulfate ion content in concrete	damaged	Stress level (3), Solution concentration (3), Immersion ways (2), Erosion age (4)	$3 \times 3 \times 2 \times 4 = 72$
Time-dependent stress-strain relationship	damaged	Stress level (3),Solution concentration (4), Immersion ways (2), Erosion age (4)	$3 \times 4 \times 2 \times 4 = 96$
Creep deformation	undamaged	Stress level (2), Solution concentration (3), Immersion ways (2),	$2 \times 3 \times 2 = 12$
Durability damage	undamaged	Stress level (3),Solution concentration (3), Immersion ways (2)	$3 \times 3 \times 2 = 18$

*Note: 1) The numbers in parentheses in the table indicate the number of factors to be considered; 2) There are 3 test pieces in each group, and the processing of test data refers to the provisions of the corresponding test specifications; 3) The creep test is equipped with a corresponding number of shrink specimens.

There are many parameters and levels considered in the experiment. To make a concise and clear presentation of the test results, the test factors are summarized and classified, as shown in Table 7.

For example, under long-term immersion, compressive stress level is 30%, sulfate solution concentration is 1%, and the erosion time is 360 days, which can be expressed as LM-S30-C1-D360.The above notation method is applicable to the whole article.

Table 7. Symbolic representation of the experimental parameters.

Experimental factors	Parameter level	Symbolic representation
Immersion ways	Long-term soaking	LM
	Dry and wet	DW
Compressive stress level	0%	S0
	15%	S15
	30%	S30
Sulfate solution concentration	1%	C1
	5%	C5
	10%	C10
Erosion age	90 days	D90
	180 days	D180
	360 days	D360
	540 days	D540

2.3. Test devices

In this paper 100 mm × 100 mm × 300 mm prismatic specimen was used. The loading apparatus is shown in Figure 1.

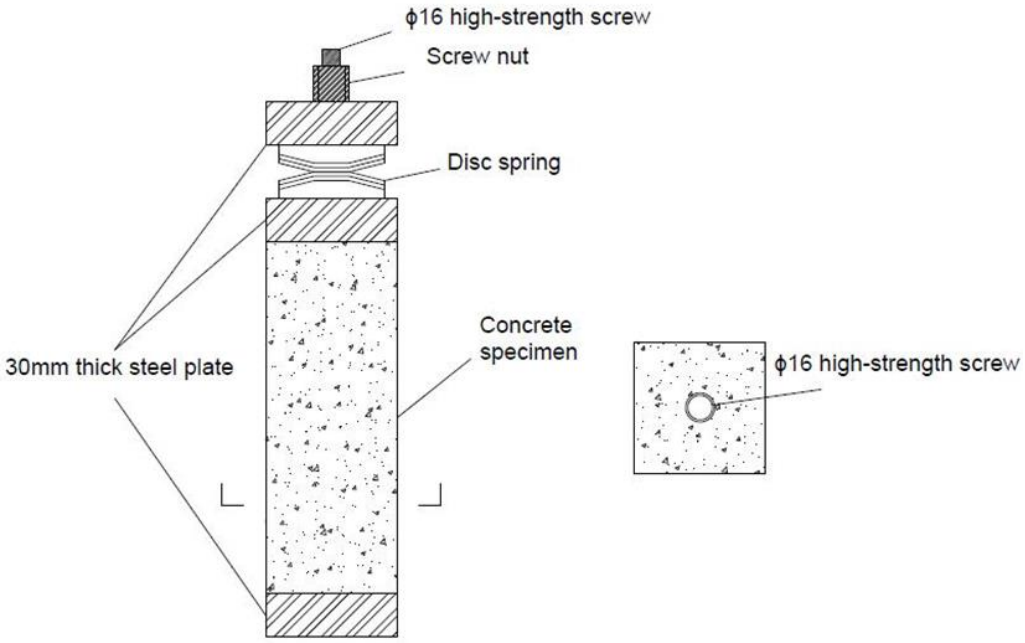

Figure 1. Loading apparatus

2.4. Experimental process

According to Standard for Test Methods of Long-term Performance and Durability of Ordinary

Concrete (GB/T50082-2009) [48], the size of the concrete specimen is 100 mm × 100 mm × 300 mm. Specimens were placed in the standard curing room (temperature 20 ± 1℃, RH above 95%). Figure 2 shows the forming and curing of some specimens.

Figure 2. Specimen casting and curing.

Under Long-term (LM) immersion, the laboratory temperature was kept at 20 ± 5 ℃, and the sodium sulfate solution was replaced once a month.

Considering the slow dry-wet alternate phenomenon in the actual environment, the dry-wet cycle system was set up, after 28 days of curing, the test piece was completely immersed in sodium sulfate solution for 8 days, and then emptied after the immersion. The test piece was dried in the container for 7 days. During drying, the temperature in the container was kept at (20 ± 2)℃, and the relative humidity is kept at (60 ± 5)% for 15 days as a cycle.

3. Modeling and discussions

3.1. CA model for simulating the diffusion process of sulfate ions in concrete

The cellular automaton used to simulate the diffusion of sulfate ions in concrete, which mainly discretizes the continuous time state into steps at certain intervals. The state of each cell in the concrete corresponds to the discrete time state. The state transition of a step is determined according to certain evolution rules, and this transition is continuously performed synchronously for each cell in the system over time, thus forming a time-varying system.

Take regular square cells for example, in a two-dimensional cellular automaton, it consists of a central cell and 4 cells located in its adjacent upper, lower, left and right directions, which is called Von Neumann-type neighbors [25]. The cell in the center will be affected in 4 directions. Assume that the side length of a single cell is δ. When concrete is separated into independent cells, sulfate ion erosion is the process of sulfate ion transfer between cells. The discrete-time diffusion process can be defined as follows [33,40,49]: from time t to time $t+\tau$, each sulfate ion in cell s jumps into its 4 neighbors along grid direction i with probability p_i (i = 1, 2, 3, 4), or stay stationary with probability $p_0 = 1 - \sum_{i=1}^{4} p_i$. Suppose that the diffusion of sulfate ions is isotropic, $p_1 = p_2 = p_3 = p_4 = p_i$, the

concentration of sulfate ions in the cell s at the time $t+\tau$ is

$$c(s,t+\tau)=c_0+p_i\left(c_1+c_2+c_3+c_4-4c_0\right) \tag{1}$$

In Eq (1), $c\left(s,t+\tau\right)$ represents the sulfate ion concentration in cell s at time $t+\tau$, $s=\left(x,y\right)$ denotes the site of cell s in the position of (x, y), so it is a location vector. c_0 is the concentration of sulfate ions in the cell s at the time t, c_1,c_2,c_3,c_4 indicate the concentration of sulfate ions in the 4 neighbors at the time t.

A Taylor expansion series expansion [40] is applied to Eq (1) can be listed as

$$\frac{\partial c(s,t)}{\partial t}+\frac{\tau}{2}\frac{\partial^2 c(s,t)}{\partial t^2}+R_2(\tau^2)=V\cdot\nabla c(s,t)+D\nabla^2 c(s,t)+R_2(\delta^2) \tag{2}$$

$c\left(s,t\right)$ represents the sulfate ion concentration in cell s at time t; D is the diffusion coefficient of sulfate ions; δ is the side length of cell, τ is the time interval for considering the cell state, they need to be assumed. The diffusion coefficient D is the most important factor to determine the speed of penetration of sulfate ions in concrete.

The diffusion coefficient of sulfate ions [40] in the CA model can be expressed as

$$D=\frac{\delta^2}{4\tau}(1-p_0)=\frac{\delta^2}{\tau}p_i \tag{3}$$

Form Eq (1), it can be seen that p_i is the key to calculating the sulfate ion concentration at a certain position. The values $p_0=1/2$ and $p_i=1/8$ can lead to a relatively good accuracy of the automaton [50], but it can still be improved. Then, p_i can be obtained by Eq (3), this will be introduced in subsequent chapters.

3.2. Sulfate ion diffusion coefficient

According to the experimental data, fitting the diffusion coefficient of sulfate ions on the surface of concrete under various test parameter combinations, the sulfate ion diffusion coefficient under various test conditions can be obtained, as shown in Tables 8 and 9.

Table 8. Diffusion coefficient of sulfate ion under the long-term immersion condition.

Immersion way	Stress level (%)	Solution concentration (%)	Erosion time (day)	C_s (%)	D (E-8cm^{2}s^{-1})	R^2
Long-term immersion	0	1	90	0.239	0.6141	0.996
			180	0.332	0.5636	0.966
			360	0.390	0.5419	0.982
			540	0.463	0.5214	0.988
		5	90	1.067	0.7036	0.959
			180	1.518	0.6759	0.947
			360	1.840	0.6256	0.984
			540	2.035	0.5981	0.993
		10	90	1.935	0.7331	0.991
			180	2.129	0.7218	0.990
			360	2.290	0.6677	0.955
			540	2.534	0.5360	0.964
	15	1	90	0.216	0.5591	0.975
			180	0.289	0.5002	0.979
			360	0.345	0.4832	0.990
			540	0.352	0.5196	0.997
		5	90	1.036	0.6649	0.960
			180	1.582	0.6325	0.946
			360	2.178	0.5633	0.978
			540	2.202	0.5726	0.974
		10	90	1.857	0.7199	0.955
			180	2.651	0.6843	0.904
			360	2.819	0.6458	0.943
			540	3.501	0.5982	0.962
	30	1	90	0.179	0.6515	0.967
			180	0.307	0.6132	0.951
			360	0.411	0.5849	0.963
			540	0.443	0.5687	0.984
		5	90	1.326	1.2802	0.920
			180	1.669	1.1644	0.907
			360	2.180	1.2186	0.956
			540	2.728	0.9224	0.988
		10	90	2.765	2.1124	0.939
			180	3.251	1.7895	0.958
			360	3.857	1.6687	0.970
			540	5.214	1.2143	0.985

Table 9. Diffusion coefficient of sulfate ion under the dry-wet condition.

Immersion way	Stress level (%)	Solution concentration (%)	Erosion time (day)	Cs (%)	D (E-8cm^{2}s^{-1})	R^2
Dry and wet cycle	0	1	90	0.276	0.7389	0.953
			180	0.375	0.7236	0.979
			360	0.405	0.6922	0.963
			540	0.499	0.6227	0.992
		5	90	1.514	1.0101	0.904
			180	1.884	0.9498	0.900
			360	1.991	1.2780	0.984
			540	2.490	1.4362	0.967
		10	90	2.849	1.4895	0.960
			180	3.259	1.3552	0.9034
			360	4.005	1.5918	0.964
			540	4.243	2.3340	0.972
	15	1	90	0.292	0.7063	0.940
			180	0.338	0.6881	0.955
			360	0.422	0.6478	0.953
			540	0.495	0.6677	0.983
		5	90	1.693	0.9107	0.974
			180	2.345	0.8444	0.957
			360	2.610	1.2925	0.980
			540	2.691	1.6116	0.985
		10	90	3.249	1.3175	0.955
			180	3.787	1.2614	0.944
			360	4.092	1.9237	0.890
			540	3.761	2.6095	0.971
	30	1	90	0.357	0.8480	0.964
			180	0.443	0.7946	0.991
			360	0.514	1.1404	0.971
			540	0.542	1.2957	0.989
		5	90	1.949	1.4593	0.946
			180	2.963	1.3170	0.962
			360	2.820	1.6883	0.965
			540	3.892	2.2956	0.981
		10	90	3.632	2.4309	0.925
			180	4.046	2.1815	0.900
			360	4.802	2.5780	0.964
			540	5.005	3.3954	0.984

From Tables 8 and 9, it can be seen that the sulfate ion diffusion coefficient obtained by regression with a certain regularity. There is a correlation with compressive stress level, solution concentration and erosion mode.

3.3. The effect of stress level and sulfate solution concentration

It is necessary to determine the relationship between the diffusion coefficient, the stress level, and the concentration of sulfate solution before the test results can be statistically analyzed. Under different erosion times and stress levels, the changing trend of the sulfate ion diffusion coefficient with solution concentration under a long-term immersion environment is shown in Figure 3.

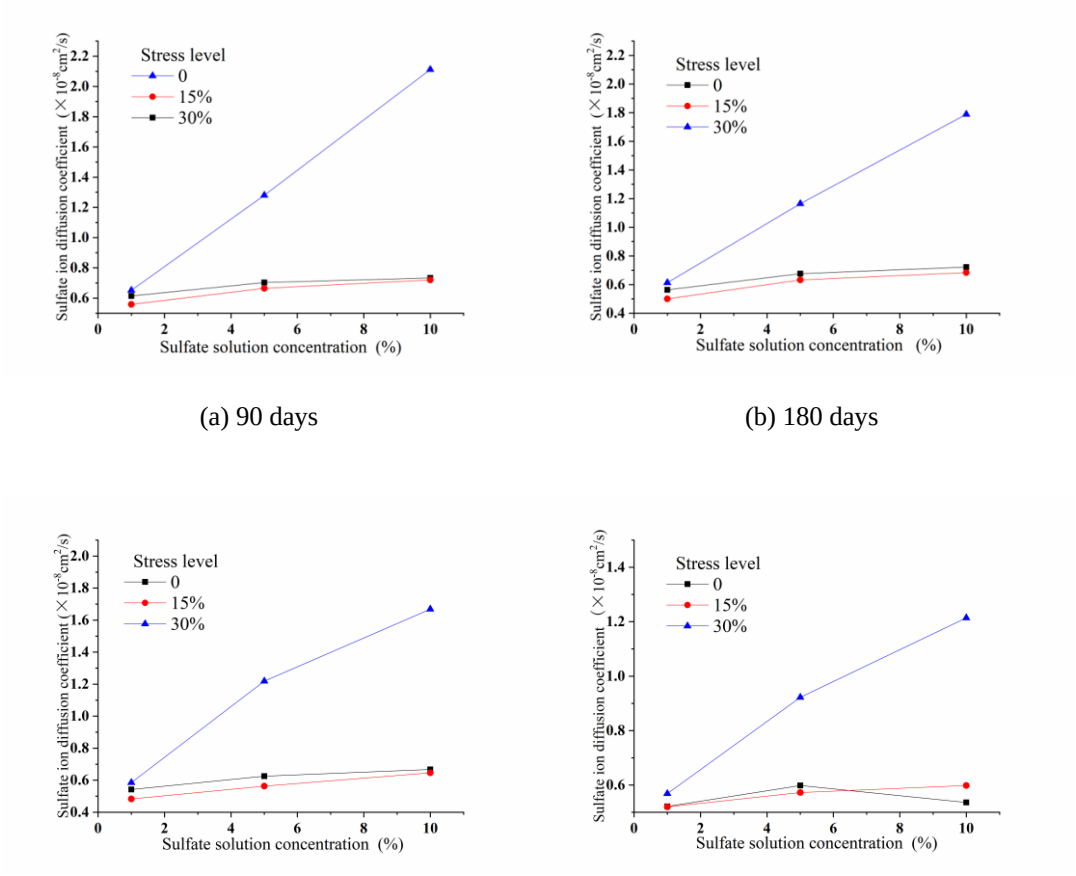

(a) 90 days (b) 180 days

(c) 360 days (d) 540 days

Figure 3. Relationship between the diffusion coefficient and concentration of sulphate solution under different stress level (LM).

It can be seen from Figure 3 that under different compressive stress levels, the sulfate solution concentration has a similar influence on the diffusion coefficient. As the solution concentration increases, the diffusion coefficient also increases, and the relationship is approximately linear.

The variation trend of sulfate ion diffusion coefficient with compressive stress level under different erosion time and solution concentration is shown in Figure 4.

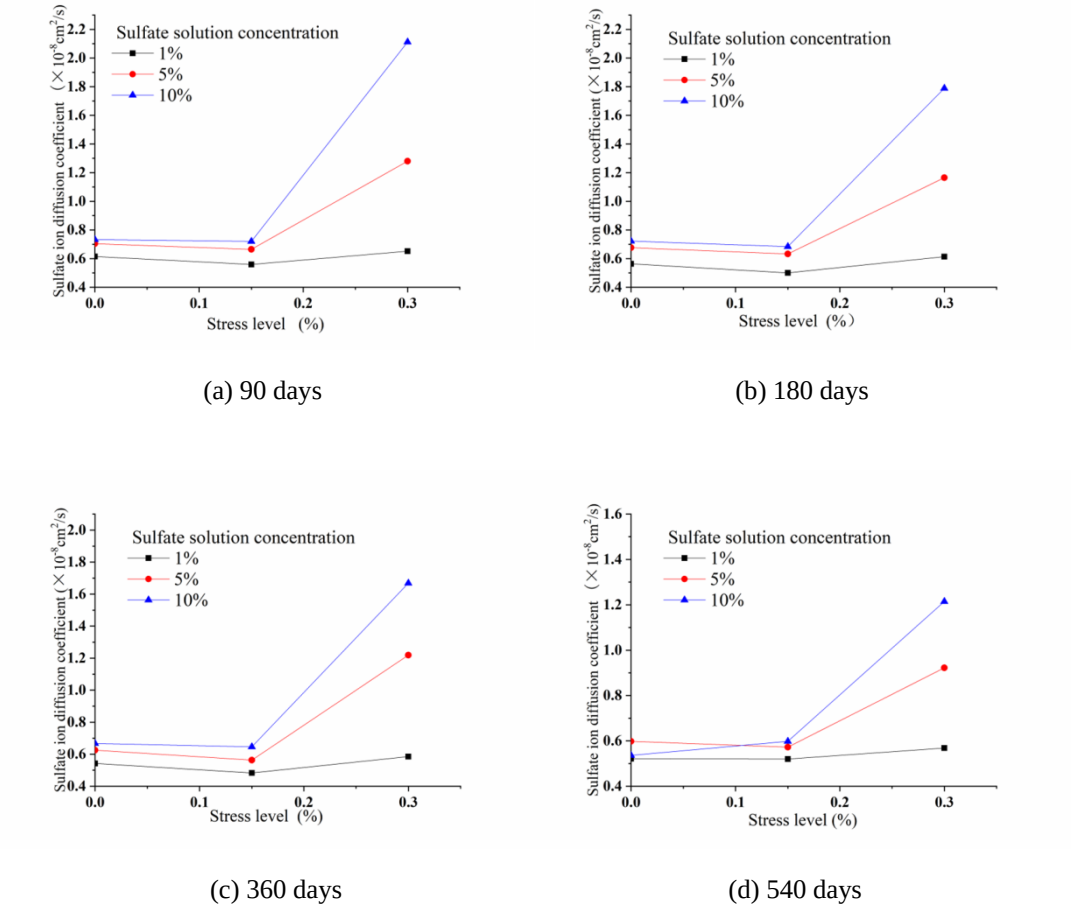

Figure 4. Relationship between the diffusion coefficient and stress level under different sulphate solution concentration (LM).

It can be seen from Figure 4 that under different solution concentrations, the stress level has similar effects on the sulfate ion diffusion coefficient and has an exponential function correlation.

Combined with Section 3.2, the diffusion coefficient D (10^{-8} cm^2s^{-1}) can be expressed as $D=f\left(\sigma / f_c, n, t\right)$, so the diffusion coefficient of sulfate ions under a long-term immersion environment can be expressed as

$$D_1=\left(a_1 \cdot n+b_1\right) \times\left\{c_1 \cdot \exp\left[d_1 \cdot\left(\sigma / f_c\right)+e_1+f_1\right]\right\} \times\left(g_1 \cdot t^{h_1}\right) \tag{4}$$

Among them, σ / f_c is the stress level (%), n is the sulfate solution concentration (%), t is the erosion time (days), and $a_1, b_1, c_1, d_1, e_1, f_1, g_1, h_1$ are the coefficients related to the test factors in the long-term immersion environment.

According to the principle of least squares method, using SPSS statistical regression software, the relationship between the sulfate ion diffusion coefficient and the test parameters in Table 8 is fitted and optimized, and the coefficients are as follows:

$$\begin{cases} a_1=0.1166, b_1=0.8678; \\ c_1=0.2574, d_1=29.1069, e_1=-7.0593, f_1=1.2754; \quad \left(R^2=0.876\right) \\ g_1=0.7506, h_1=-0.1690 \end{cases} \tag{5}$$

It can be seen from the value of the degree of fit R^2 that the above coefficients have a fitting effect.

Similar to the analysis of the relationship between sulfate ion diffusion coefficient and test factors under long-term immersion, in this experiment, the variation trend of sulfate ion diffusion coefficient with solution concentration under different erosion times and stress levels under dry -wet cycles is shown in Figure 5.

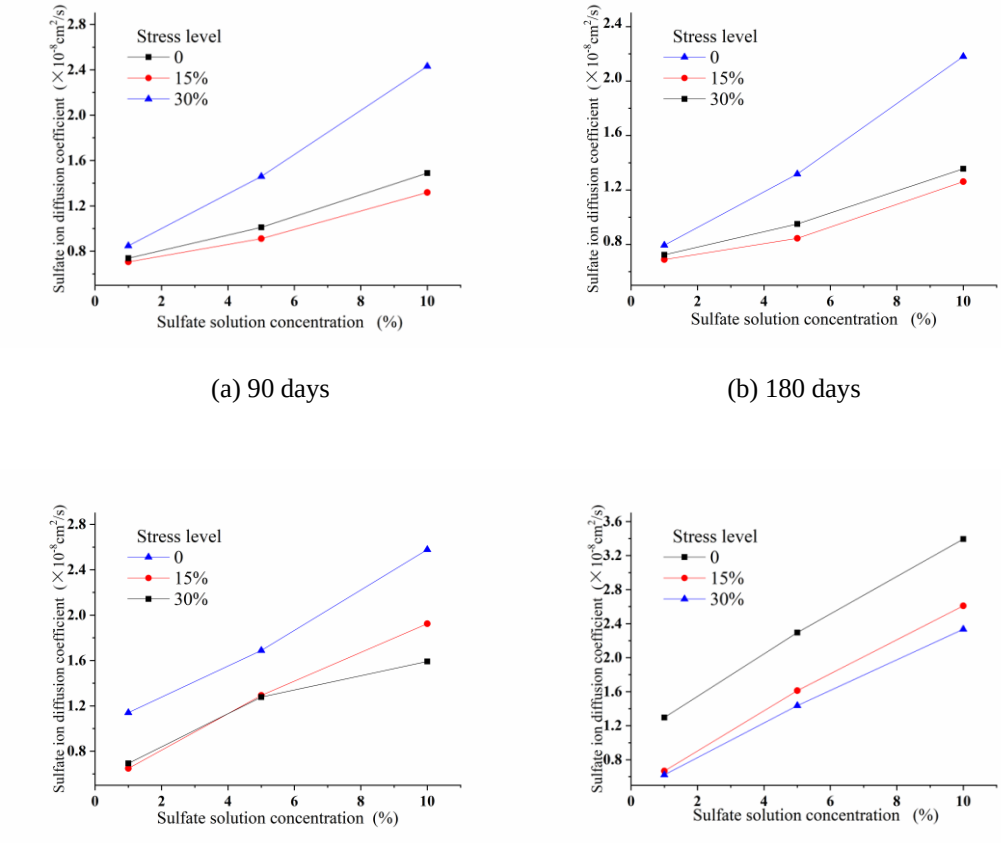

(a) 90 days (b) 180 days

(c) 360 days (d) 540 days

Figure 5. Relationship between the diffusion coefficient and concentration of sulphate solution under different stress level (DW).

The variation trend of the sulfate ion diffusion coefficient with the stress level under different erosion time and solution concentration is shown in Figure 6.

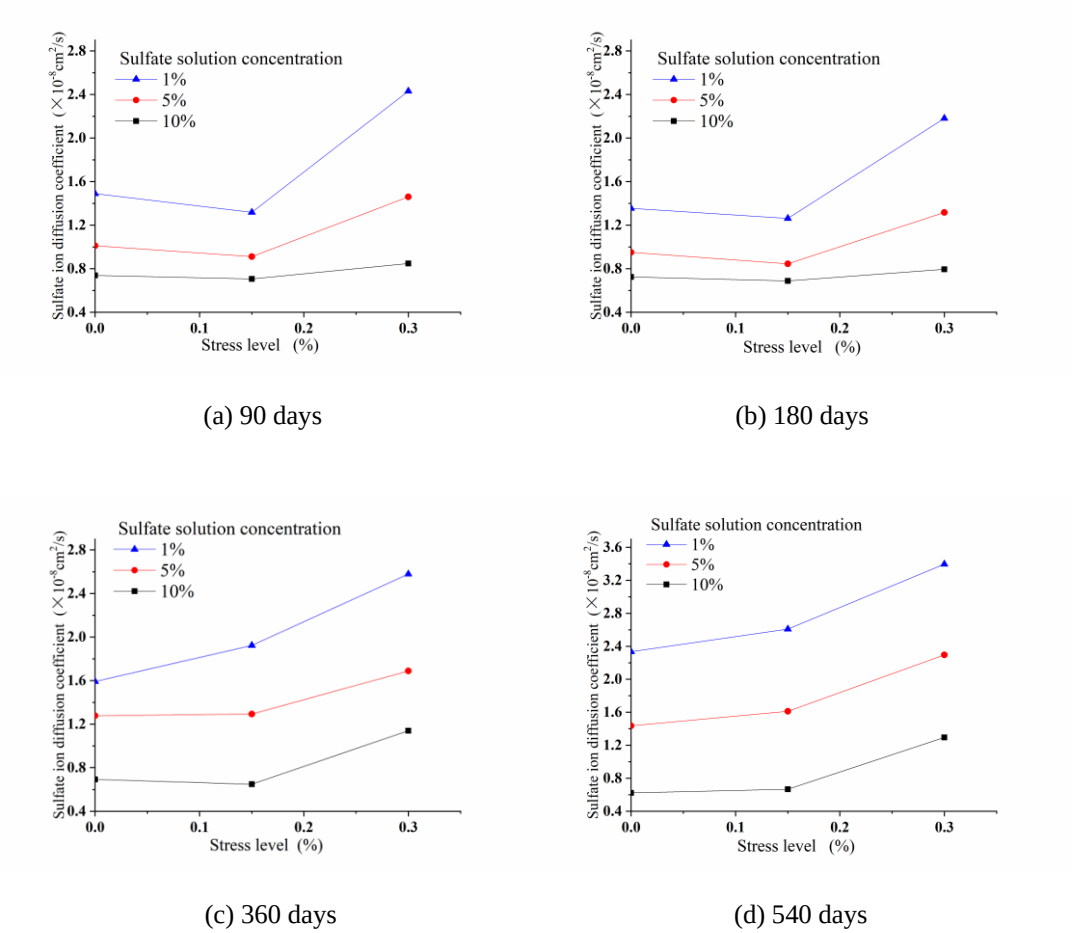

Figure 6. Relationship between the diffusion coefficient and stress level under different sulphate solution concentration (DW).

It can be seen from Figures 5 and 6 that the relationship between the sulfate ion diffusion coefficient and the solution concentration and stress level under the dry-wet cycle is consistent with the long-term immersion. Therefore, the diffusion coefficient of sulfate ions in concrete under the action of wet and dry cycles can be expressed as

$$D_2=\left(a_2\cdot n+b_2\right)\times\left\{c_2\cdot\exp\left[d_2\cdot\left(\sigma/f_c\right)+e_2+f_2\right]\right\}\times\left(g_2\cdot t^{h_2}\right) \tag{6}$$

Among them, $a_2, b_2, c_2, d_2, e_2, f_2, g_2, h_2$ are the coefficients related to test factors under the environment of the dry-wet cycle system.

Fitting the relationship between the sulfate ion diffusion coefficient and the test parameters in Table 9, the coefficients are as follows

$$\begin{cases} a_2=0.1859, b_2=0.8500; \\ c_2=0.1641, d_2=15.6538, e_2=-5.3488,\ f_2=0.1611; \quad (R^2=0.915) \\ g_2=0.8617, h_2=0.2737 \end{cases} \tag{7}$$

It can be seen from formulas (5) and (7) that the fitting coefficient h is quite different. In formula (5), $h_1<0$, indicating that the erosion time is a negative exponential function of the diffusion coefficient in a long-term immersion, the diffusion coefficient decreases exponentially with the increase of erosion

time; in formula (7) , $h_2 > 0$, indicating that the erosion time is a positive exponential function of the diffusion coefficient in a long-term immersion, the diffusion coefficient increases exponentially with the increase of erosion time.

3.4. Improved model

It can be found from the above that the sulfate ion diffusion coefficient D is relevant to stress level, sulfate solution concentration, immersion ways and corrosion time, p_i can be obtained from the sulfate ion diffusion coefficient D. Considering the jump probabilities p_i varying with stress level, sulfate solution concentration, immersion ways and corrosion time, the MPCA model obtained by the combination of Eqs (3), (5) and (7).

4. Results and disscussion

The comparison between the MPCA model and some experimental data are shown in Figure 7 to Figure 14.

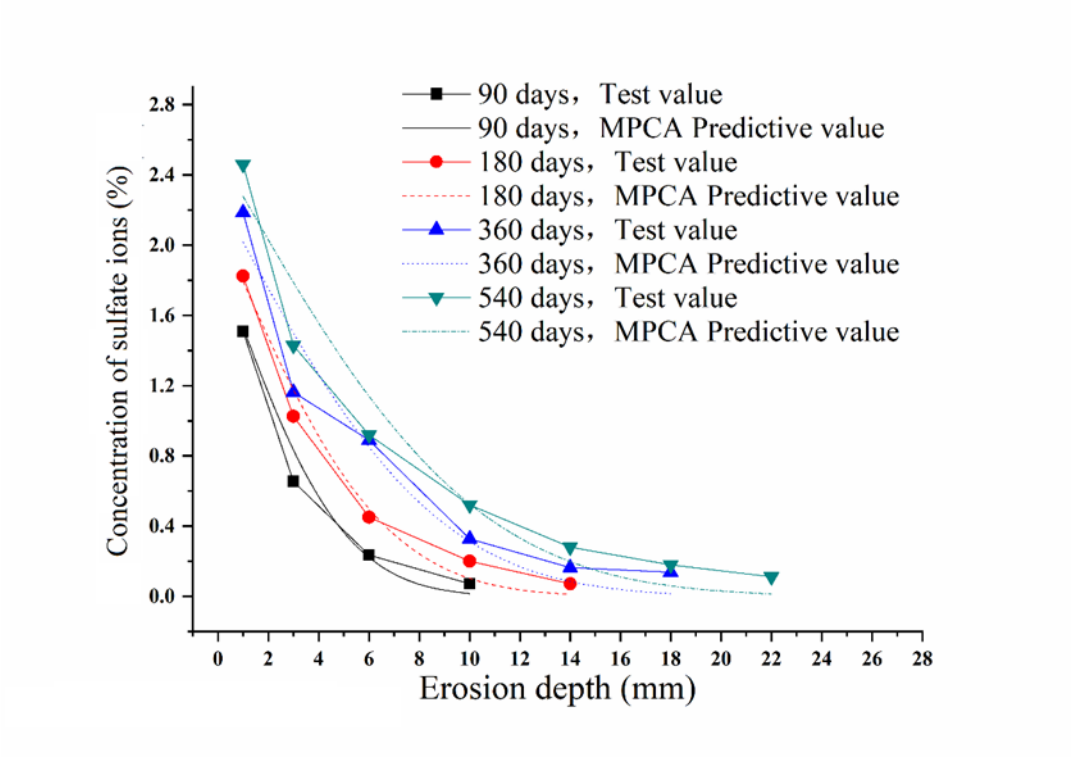

Figure 7. Comparison of the experimental data and the calculation of MPCA under LM-S0-C10.

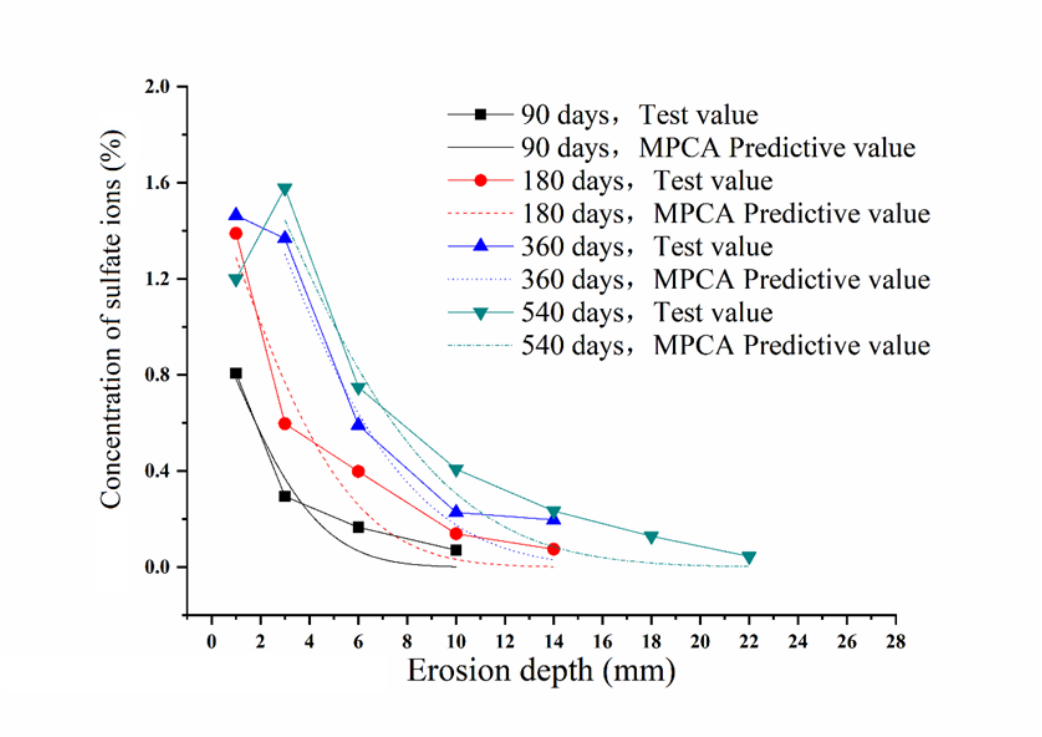

Figure 8. Comparison of the experimental data and the calculation of MPCA under LM-S15-C5.

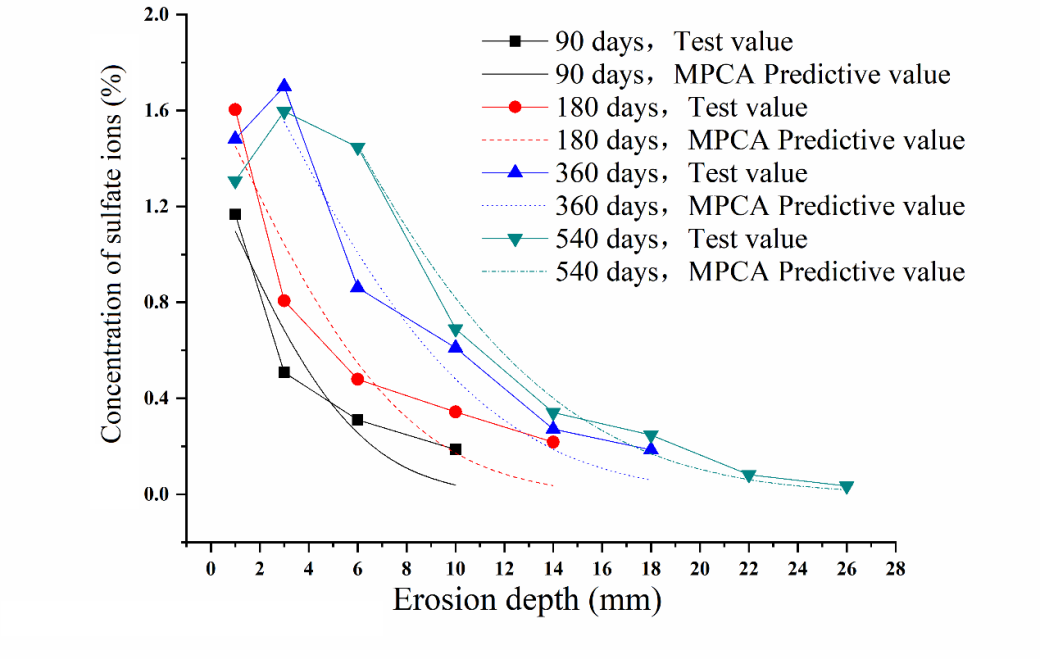

Figure 9. Comparison of the experimental data and the calculation of MPCA under LM-S30-C5.

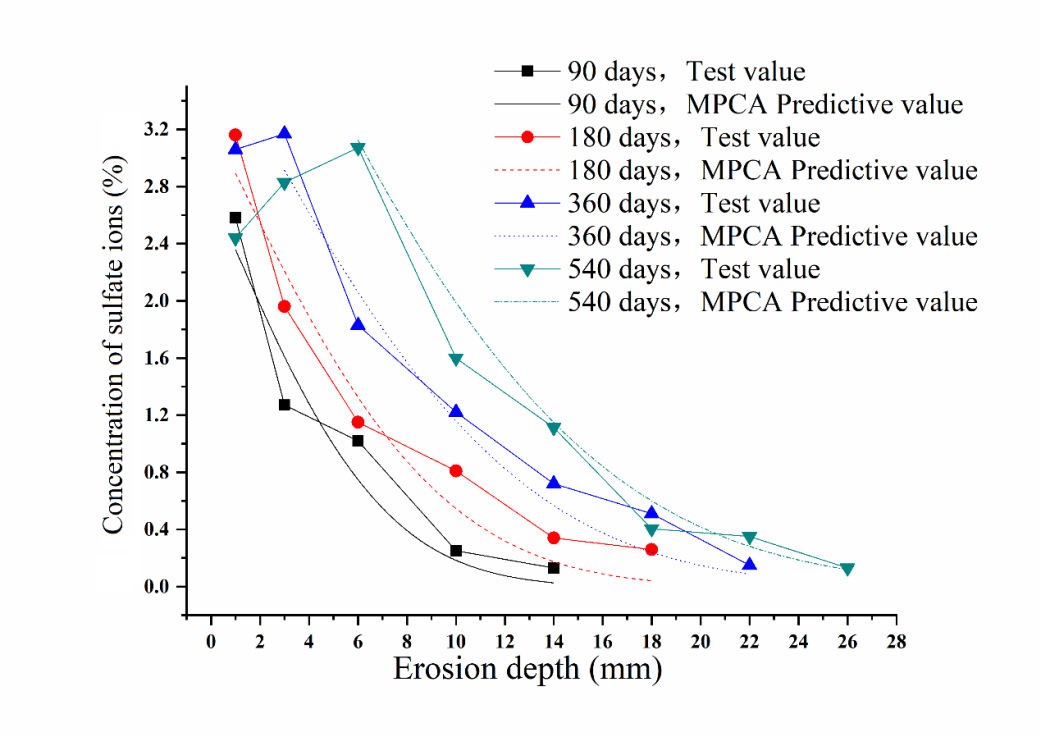

Figure 10. Comparison of the experimental data and the calculation of MPCA under LM-S30-C10.

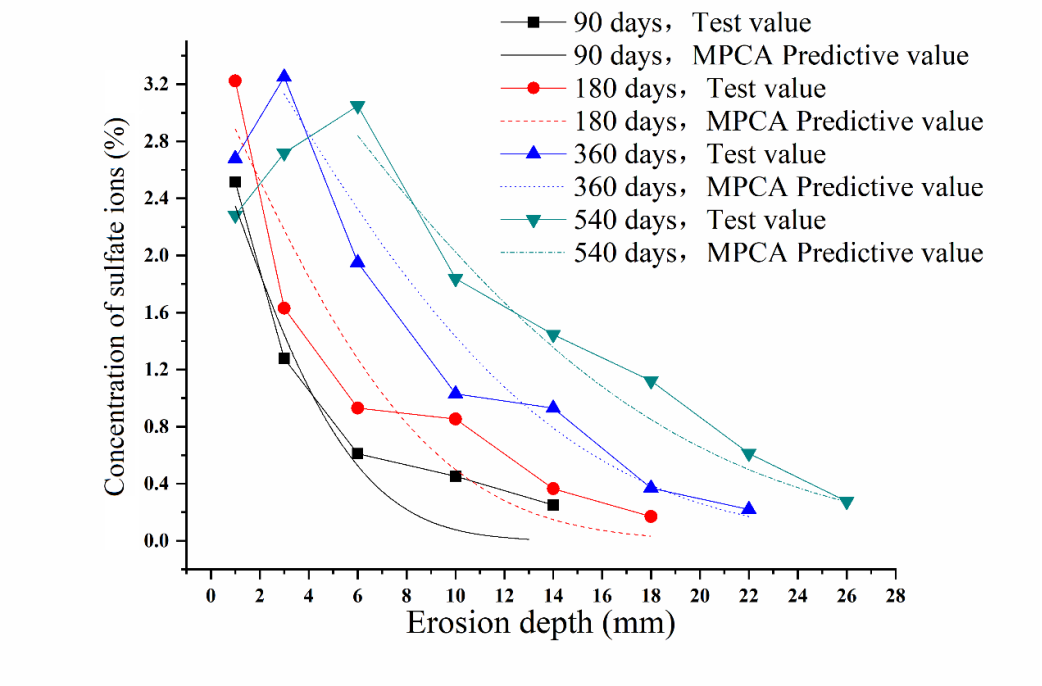

Figure 11. Comparison of the experimental data and the calculation of MPCA under DW-S0-C10.

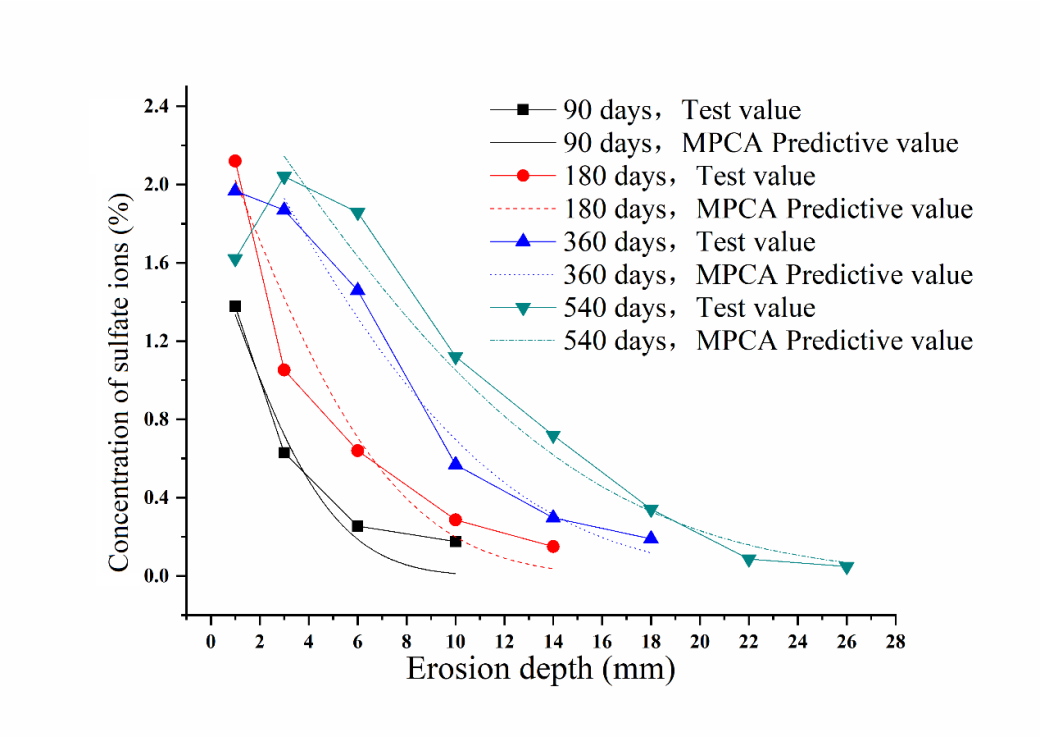

Figure 12. Comparison of the experimental data and the calculation of MPCA under DW-S15-C5.

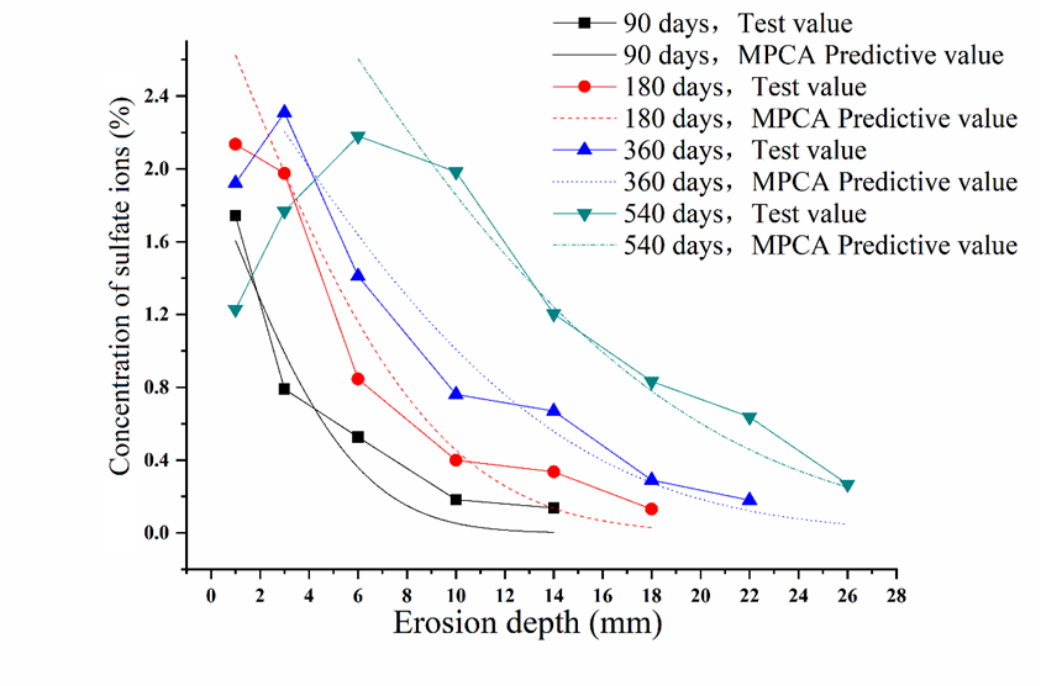

Figure 13. Comparison of the experimental data and the calculation of MPCA under DW-S30-C5.

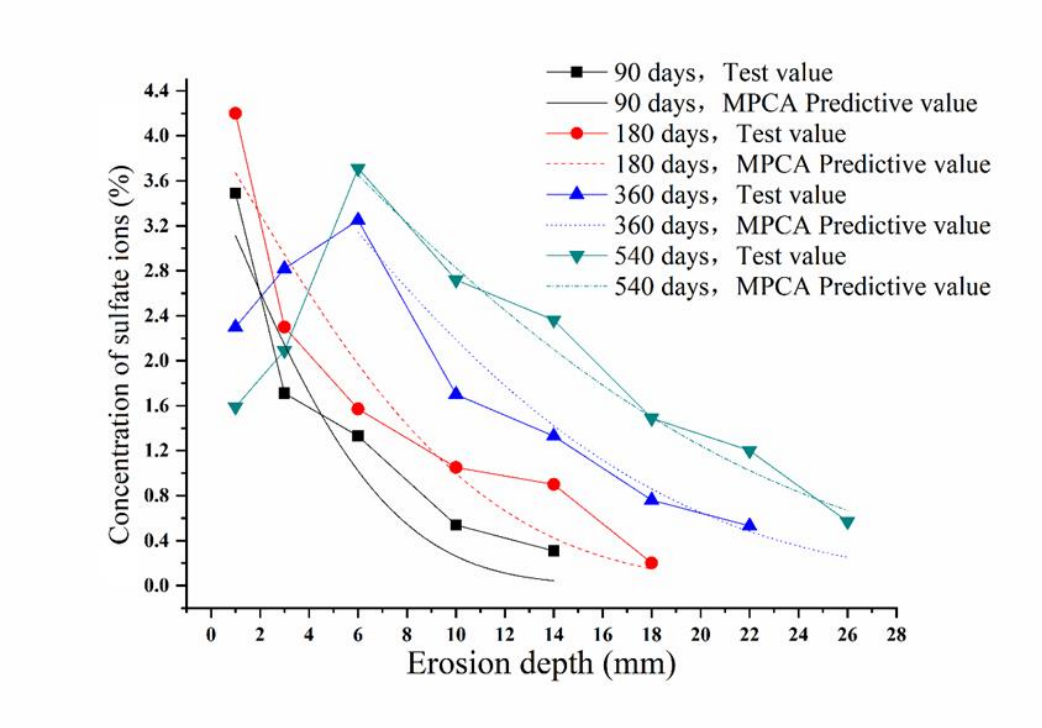

Figure 14. Comparison of the experimental data and the calculation of MPCA under DW-S30-C10.

From Figures 7–14, the sulfate ion concentration in the concrete decreased with the increase of erosion depth. Firstly, sulfate ions entered the pores of concrete. And then, under the action of the solution concentration gradient, sulfate ions were transmitted to the inside of concrete relied on effects of diffusion, penetration and capillary absorption. During the transmission, a series of chemical reactions between sulfate ions and the hydration products in the concrete were also produced. The products of these reactions formed on the outer layer of concrete and the pores were partially filled. The transmitting procedure of sulfate ions was slowed down and a transmitting gradient was formed. In addition, except for the surface layer, under the same erosion depth, the content of sulfate ions in each layer of concrete increased with the increase of erosion time. It can be proved that the transmitting procedure of sulfate ions proceeded with the erosion time.

Sulfate attack will cause damage to concrete. The diffusion of sulfate ion mainly depends on the concentration difference of solution to form concentration gradient. Therefore, in high concentration sulfate solution, the deeper the concrete sample is eroded. The wet and dry cycle accelerates the transport of sulfate ions in concrete. In wet state, the continuous transmission of sulfate ions from outer layer to inner layer is caused by gradient of sulfate solution concentration at different concrete depths. In dry state, the dispersion of water in concrete results in the increase of sulfate concentration in pore. Due to the evaporation of water in outer layer and the high content of raw sulfate ions in outer layer, the concentration of outer sulfate solution is higher, which accelerates the transmission of sulfate ions into concrete. On the other hand, the accelerated transmission process also accelerates the sulfate attack process of concrete, expands the existing defects and pores in concrete, and develops the inherent cracks and cracks in concrete from discontinuous state to connected state. Gypsum and AFt produced by the reaction between sulfate ion and cement hydration products are expansive products. With the deepening of erosion process, these expansive products cause tensile

stress in concrete, which causes rapid opening of micro-cracks in concrete, accelerates the connection of defects such as pore and crack in concrete, and enhances the permeability of concrete. It provides a good channel for further diffusion and penetration of sulfate ions into concrete, resulting in increased corrosion products and sulfate ions at the same erosion depth.

The content of sulfate ions at an erosion depth of 1 mm was lower than at an erosion depth of 3 mm, and the content of sulfate ions at an erosion depth of 1 mm or 3 mm was lower than at an erosion depth of 6 mm. This phenomenon could be explained that under the effect of dry-wet cycles or high-concentration sulfate solutions, the surface of concrete was peeled off with the erosion time, leading to sulfate ions decreased. However, for long-term immersion, low solution concentration, and short erosion time, this phenomenon did not exist.

At the state of 15% compressive stress level, due to the existence of compressive stress, the interior of concrete was squeezed to a certain extent. The initial compaction effect would slow the diffusion of sulfate ions in the concrete. The comparison with the unloading state showed that the content of sulfate ions under the long-term immersion decreased at the initial stage of the erosion with the same erosion time and erosion depth. As the erosion time increased, when at the 5% concentration, erosion time was 360 days, the content of sulfate ions increased. When the concentration of sulfate solution was 10%, this phenomenon was advanced to 180 days. Under the dry-wet cycle, when the concentration of sulfate solution was 1%, due to the acceleration effect of the dry-wet cycle and the compaction effect of the pressure load, the content of sulfate ions in concrete was slightly higher than the test result without load. But the content of sulfate ions in concrete was significantly higher than the test result which under unloading and long-term immersion. When the concentrations of sulfate solution were 5 and 10%, the content of sulfate ions in concrete increased significantly.

At the state of 30% compressive stress level, the effect of load intensified the erosion process of sulfate. In a long-term immersion environment, compared with the unloading state, when the concentration solution was 1%, it was found that the content of sulfate ions increased at the erosion time of 360 days. When the concentration solutions were 5 and 10%, the content of sulfate ions significantly increased at each erosion time. The transmitting process of sulfate ions developed rapidly under the coupling effect of the dry-wet cycle and compression load. Compared with the unloading and the 15% stress levels, the content of sulfate ions increased significantly, and the surface concrete was severely corroded and peeled off.

The comparison with the test value showed that the calculated value of the model was in good agreement with the test value. When the erosion time was 90 days, the calculated values of the MPCA model was slightly smaller than the experimental value after the sulfate ion erodes the concrete to a depth greater than 6 mm. This situation also manifested when the erosion time was 180 days. It can be explained that the concrete was due to the existence of aggregate and pores which caused the non-isotropic diffusion of sulfate ions in concrete, and MPCA was based on the assumption of sulfate ions diffuse isotropically in concrete. The anisotropy of the diffusion was more obvious at the erosion depth larger than 6mm in concrete. When the erosion time were 360 days and 540 days, the calculated values of the MPCA model were in good agreement with the experimental values, indicating that with the erosion time increased, the anisotropic effect of sulfate ions diffusion in the concrete gradually weakened, and in each section of concrete, the content of sulfate ions tended to be uniform.

In addition, experimental data from other researchers [11,51,52] were also used to verify the

MPCA, as shown in Figures 15–17.

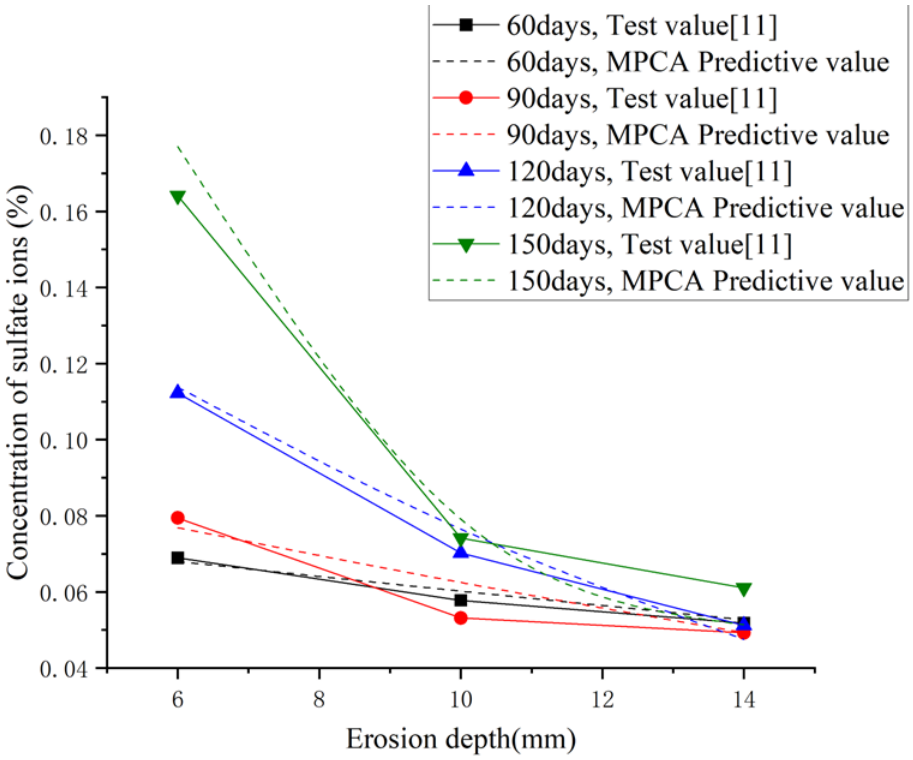

Figure 15. Comparison of the experimental data and the calculation of MPCA under LM-S0-C5 [11].

In Figure 15, under long-term immersion and 5% sulfate solution, when the erosion time was 60 days, the concentrations of sulfate ions were 0.0689% at 6 mm, 0.0578% at 10 mm, 0.0519% at 14 mm, the predictive values were 0.0680%, 0.0602%, 0.0527%. When the erosion time was 90 days, the concentrations of sulfate ions were 0.0794% at 6 mm, 0.0532% at 10 mm, 0.0492% at 14mm, the predictive values were 0.0769%, 0.0625%, 0.0493%. When the erosion time was 120 days, the concentrations of sulfate ions were 0.1123% at 6 mm, 0.0702% at 10 mm, 0.0512% at 14mm, the predictive values were 0.1138, 0.0765 and 0.0475%. When the erosion time was 150 days, the concentrations of sulfate ions were 0.1641% at 6 mm, 0.0742% at 10 mm, 0.0611% at 14mm, the predictive values were 0.1770, 0.0791 and 0.0514%.

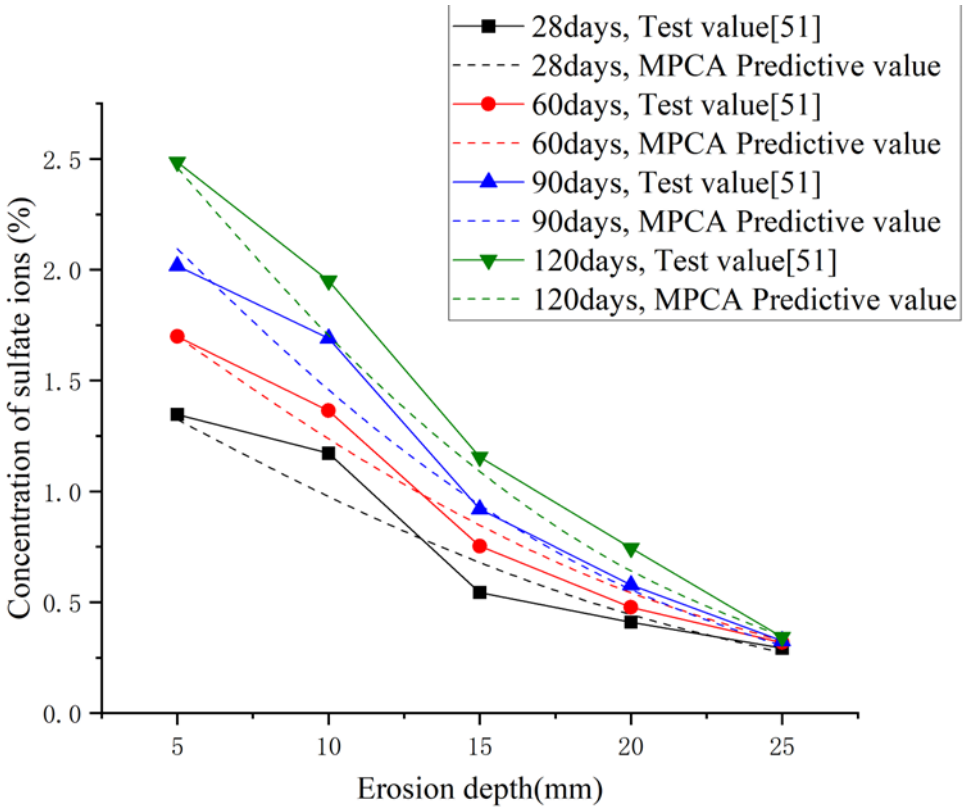

Figure 16. Comparison of the experimental data and the calculation of MPCA under LM-S0-C5 [51].

In Figure 16, when the erosion time was 28 days, the concentrations of sulfate ions were 1.3473% at 5 mm, 1.1716% at 10 mm, 0.5439% at 15mm, 0.4100% at 20 mm, 0.2929% at 25 mm, the predictive values were 1.3242, 0.9767, 0.6796, 0.4446 and 0.2728%. When the erosion time was 60 days, the concentrations of sulfate ions were 1.6987% at 5 mm, 1.3640% at 10 mm, 0.7531% at 15mm, 0.4770% at 20 mm, 0.3180% at 25mm, the predictive values were 1.6988, 1.2376, 0.8471, 0.5430 and 0.3250%. When the erosion time was 90 days, the concentrations of sulfate ions were 2.0167% at 5 mm, 1.6903% at 10 mm, 0.9205% at 15mm, 0.5774% at 20 mm, 0.3264% at 25mm, the predictive values were 2.0948, 1.4581, 0.9392, 0.5573 and 0.3035%. When the erosion time was 120 days, the concentrations of sulfate ions were 2.4854% at 5 mm, 1.9498% at 10 mm, 1.1548% at 15mm, 0.7448% at 20 mm, 0.3431% at 25mm, the predictive values were 2.4606, 1.7044, 1.0905, 0.6416 and 0.3459%.

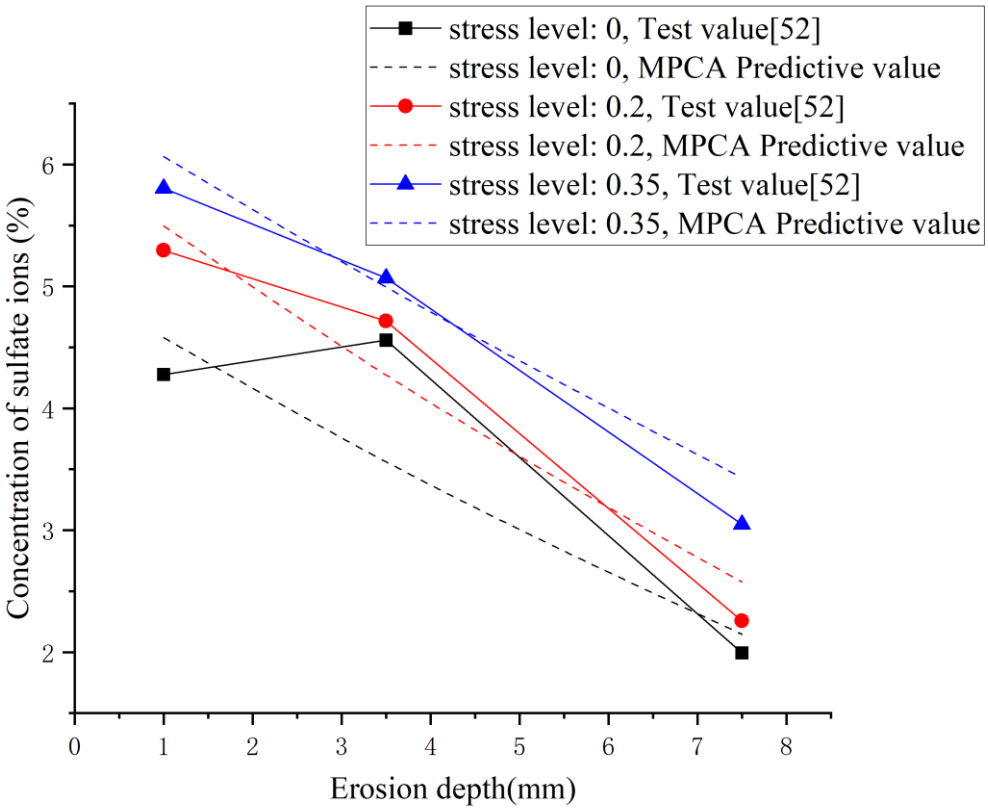

Figure 17. Comparison of the experimental data and the calculation of MPCA with different stress level at 180 days under DW-C10 [52].

In Figure 17, under dry-wet cycles and 10% sulfate solution, when stress level was 0, the concentrations of sulfate ions were 4.2775% at 1 mm, 4.5586% at 3.5 mm, 1.9942% at 7.5mm, the predictive values were 4.5803, 3.5609 and 2.1460%. When stress level was 0.2, the concentrations of sulfate ions were 5.2963% at 1 mm, 4.7166% at 3.5 mm, 2.2576% at 7.5mm, the predictive values were5.4963, 4.2731 and 2.5751%. When stress level was 0.35, the concentrations of sulfate ions were 5.8056% at 1 mm, 5.0679% at 3.5 mm, 3.0480% at 7.5mm, the predictive values were 6.0641, 4.9942 and 3.4315%.

From the above comparison results, it can be found that the values calculated by the MPCA model are in good agreement with the experimental values, which indicates the universality of the MPCA model. Therefore, the MPCA model can effectively simulate the erosion process of sulfate ions under load and different immersion ways.

5. Conclusions

The test results showed that the dry-wet cycle accelerated the diffusion process of sulfate ions in concrete. With the concentration of solution and the erosion time increased, the degree of concrete erosion would become more severe. When load existed, under the 15% stress level, the initial compressive stress made the interior of the concrete tighter and slowed the diffusion of sulfate ions, while the 30% stress level accelerated the diffusion of sulfate ions.

Based on the basic principles of CA, the evolution rules of the cellular state were depicted for

the simulation analysis to the diffusion of sulfate ions in concrete. The cell state evolution rules of the model conformed to the sulfate ion diffusion mechanism and can reflect the essential characteristics of the diffusion process of sulfate ions in concrete.

With the experimental data, MPCA model was established. This model took into account the effects of stress level, the concentration of sulfate solution, and erosion methods on the sulfate ion diffusion coefficient. The comparison with the experimental results shows that the applicability of model was well.

Acknowledgments

The authors would like to acknowledge the financial support of the National Natural Science Foundation of China (52168030).

Conflict of interest

The authors declare there is no conflict of interest.

References

1. Y. Chen, P. Liu, Z. W. Yu, Study on degradation of macro performances and microstructure of concrete attacked by sulfate under artificial simulated environment, *Constr. Build. Mater.*, **260** (2020), 119951. https://doi.org/10.1016/j.conbuildmat.2020.119951
2. N. Zhao, S. L. Wang, X. Y. Quan, F. Xu, K. N. Liu, Y. Liu, Behavior of polyvinyl alcohol fiber reinforced geopolymer composites under the coupled attack of sulfate and freeze-thaw in a marine environment, *Ocean Eng.*, **238** (2021), 109734. https://doi.org/10.1016/j.oceaneng.2021.109734
3. Y. Chen, J. F. Davalos, I. Ray, H. Y. Kim, Accelerated aging tests for evaluations of durability performance of FRP reinforcing bars for concrete structures, *Compos. Struct.*, **78** (2007), 101–111. https://doi.org/10.1016/j.compstruct.2005.08.015
4. A. E. Idiart, C. M. López, I. Carol, Chemo-mechanical analysis of concrete cracking and degradation due to external sulfate attack: A meso-scale model, *Cem. Concr. Compos.*, **33** (2011), 411–423. https://doi.org/10.1016/j.cemconcomp.2010.12.001
5. D. D. Sun, K. Wu, H. S. Shi, S. Miramini, L. H. Zhang, Deformation behaviour of concrete materials under the sulfate attack, *Constr. Build. Mater.*, **210** (2019), 232–241. https://doi.org/10.1016/j.conbuildmat.2019.03.050
6. J. Marchand, E. Samson, Y. Maltais, J. J. Beaudoin, Theoretical analysis of the effect of weak sodium sulfate solutions on the durability of concrete, *Cem. Concr. Compos.*, **243** (2002), 317–329. https://doi.org/10.1016/S0958-9465(01)00083-X
7. R. Tixier, B. Mobasher, Modeling of damage in cement-based materials subjected to external sulfate attack, I: Formulation, *J. Mater. Civ. Eng.*, **15** (2003), 305–313. https://doi.org/10.1061/(ASCE)0899-1561(2003)15:4(305)
8. R. Tixier, B. Mobasher, Modeling of damage in cement-based materials subjected to external sulfate attack, II: Comparision with experiments, *J. Mater. Civ. Eng.*, **15** (2003), 314–322. https://doi.org/10.1061/(ASCE)0899-1561(2003)15:4(314)

9. B. Bary, Simplified coupled chemo-mechanical modeling of cement pastes behavior subjected to combined leaching and external sulfate attack, *Int. J. Numer. Anal. Meth. Geomech*, **32** (2008), 1791–1816. https://doi.org/10.1002/nag.696|
10. S. Sarkar, S. Mahadevan, J. C. L. Meeussen, H. van der Sloot, D. S. Kosson, Numerical simulation of cementitious materials degradation under external sulfate attack, *Cem. Concr. Compos.*, **32** (2010), 241–252. https://doi.org/10.1016/j.cemconcomp.2009.12.005
11. C. Sun, J. K. Chen, J. Zhu, M. H. Zhang, J. Ye, A new diffusion model of sulfate ions in concrete, *Constr. Build. Mater.*, **39** (2013), 39–45. https://doi.org/10.1016/j.conbuildmat.2012.05.022
12. T. Ikumi, S. H. P. Cavalaro, I. Segura, A. Fuente, A. Aguado, Simplified methodology to evaluate the external sulfate attack in concrete structures, *Mater. Des.*, **89** (2016), 1147–1160. https://doi.org/10.1016/j.matdes.2015.10.084
13. D. D. Sun, K. Wu, H. S. Shi, L. T. Zhang, L. H. Zhang, Effect of interfacial transition zone on the transport of sulfate ions in concrete, *Constr. Build. Mater.*, **192** (2018), 28–37. https://doi.org/10.1016/j.conbuildmat.2018.10.140
14. Z. Chen, L. Y. Wu, V. Bindiganavile, C. F. Yi, Coupled models to describe the combined diffusion-reaction behaviour of chloride and sulphate ions in cement-based systems, *Constr. Build. Mater.*, **243** (2020), 118232. https://doi.org/10.1016/j.conbuildmat.2020.118232
15. Y. W. Zhou, H. Tian, L. L. Sui, F. Xing, N. X. Han, Strength deterioration of concrete in sulfate environment: An experimental study and theoretical modeling, *Adv. Mater. Sci. Eng.*, **2015** (2015), 1–13. https://doi.org/10.1155/2015/951209
16. P. Liu, Y. Chen, Z. W. Yu, Z. H. Lu, Effect of sulfate solution concentration on the deterioration mechanism and physical properties of concrete, *Constr. Build. Mater.*, **227** (2019), 116641. https://doi.org/10.1016/j.conbuildmat.2019.08.022
17. S. W. Tang, Y. Yao, C. Andrade, Z. J. Li, Recent durability studies on concrete structure, *Cem. Concr. Res.*, **78** (2015), 143–154. https://doi.org/10.1016/j.cemconres.2015.05.021
18. M. Santhanam, M. Otieno, Deterioration of concrete in the marine environment, *Marine Concr. Struct.*, (2016), 137–149. https://doi.org/10.1016/B978-0-08-100081-6.00005-2
19. A.M. Neville, Recovery of creep and observations on the mechanism of creep of concrete, *Appl. Sci. Res.*, **9** (1960). https://doi.org/10.1007/BF00382191
20. J. P. Li, F. Xie, G. W. Zhao, L. Li, Experimental and numerical investigation of cast-in-situ concrete under external sulfate attack and drying-wetting cycles, *Constr. Build. Mater.*, **249** (2020), 118789. https://doi.org/10.1016/j.conbuildmat.2020.118789
21. P. J. Tumidajski, G. Chan, K. E. Philipose, An effective diffusivity for sulfate transport into concrete, *Cem. Concr. Res.*, **25** (1995), 1159–1163. https://doi.org/10.1016/0008-8846(95)00108-O
22. P. N. Gospodinov, Numerical simulation of 3D sulfate ion diffusion and liquid push out of the material capillaries in cement composites, *Cem. Concr. Res.*, **35** (2005), 520–526. https://doi.org/10.1016/j.cemconres.2004.07.005
23. G. J. Yin, X. B. Zuo, Y. J Tang, O. Ayinde, J. L. Wang, Numerical simulation on time-dependent mechanical behavior of concrete under coupled axial loading and sulfate attack, *Ocean Eng.*, **142** (2017), 115–124. https://doi.org/10.1016/j.oceaneng.2017.07.016
24. W. Sun, X. B. Zuo, Numerical simulation of sulfate diffusivity in concrete under combination of mechanical loading and sulfate environments, *J. Sustainable Cem.-Based Mater.*, **1** (2012), 46–55. https://doi.org/10.1080/21650373.2012.728564

25. J. Von Neumann, Theory of self-reproducing automata, University of Illinois press, Urbana, 1966.
26. S. Wolfram, Statistical mechanics of cellular automata, *Rev. Mod. Phys.*, **55** (1983), 601–644. https://doi.org/10.1103/RevModPhys.55.601
27. A. Talaminos-Barroso, J. Reina-Tosina, L. M. Roa-Romero, Models based on cellular automata for the analysis of biomedical systems, *Control Appl. Biomed. Eng. Syst.*, (2020), 405–445. https://doi.org/10.1016/B978-0-12-817461-6.00014-7
28. W. C. Huang, B. W. Zhou, Y. C. Yu, D. Z. Yin, Vulnerability analysis of road network for dangerous goods transportation considering intentional attack: Based on cellular automata, *Reliab. Eng. Syst. Saf.*, **214** (2021), 107779. https://doi.org/10.1016/j.ress.2021.107779
29. S. Ghosh, S. Bhattacharya, Computational model on COVID-19 pandemic using probabilistic cellular automata, *SN Comput. Sci.*, **230** (2021). https://doi.org/10.1007/s42979-021-00619-3
30. Y. Z. X. Liu, J. Q. Guo, J. Taplin, Y. B. Wang, Characteristic analysis of mixed traffic flow of regular and autonomous vehicles using cellular automata, *J. Adv. Transp.*, **2017** (2017), 1–10. https://doi.org/10.1155/2017/8142074
31. K. Małecki, A computer simulation of traffic flow with on-street parking and drivers' behaviour based on cellular automata and a multi-agent system, *J. Comput. Sci.*, **28** (2018), 32–42. https://doi.org/10.1016/j.jocs.2018.07.005
32. F. Biondini, F. Bontempi, D. M. Frangopol, P. G. Malerba, Durability analysis of deteriorating concrete structures due to diffusion processes: Application to box-girder bridges, in *Proceedings of the International Conference on Short and Medium Span Bridges*, **2** (2002),745–752.
33. F. Biondini, F. Bontempi, D. M. Frangopol, P. G. Malerba, Cellular automata approach to durability analysis of concrete structures in aggressive environments, *J. Struct. Eng.*, **130** (2004), 1724–1737. https://doi.org/10.1061/(ASCE)0733-9445(2004)130:11(1724)
34. F. Biondini, F. Bontempi, D. M. Frangopol, A cellular automata finite element formulation for lifetime assessment of concrete structures. in *Proceedings of the Structural Engineers World Congress*, 2002.
35. F. Biondini, D. M. Frangopol, P. G. Malerba, Uncertainty effects on lifetime structural performance of cable-stayed bridges, *Probabilistic Eng. Mech.*, **23** (2008). https://doi.org/10.1016/j.probengmech.2008.01.008
36. F. Biondini, D. M. Frangopol, Probabilistic life-cycle optimization of concrete structures, *Engineering*, 2008.
37. J. Podroužek, Importance sampling strategy for oscillatory stochastic processes, in *5th International Conference on Reliable Engineering Computing*, 2012.
38. F. Biondini, D. M. Frangopol, Probabilistic limit analysis and lifetime prediction of concrete structures, *Struct. Infrastruct. Eng.*, **4** (2008), 399–412. https://doi.org/10.1080/15732470701270157
39. D. Vořechovská, J. Podroužek, M. Chromá, P. Rovnaníková, B. Teplý, Modeling of chloride concentration effect on reinforcement corrosion, *Comput-Aided. Civ. Inf.*, **24** (2009), 446–458. https://doi.org/10.1111/j.1467-8667.2009.00602.x|
40. J. Cao, Y. F. Wang, K. P. Li, Y. S. Ma, Modeling the diffusion of chloride ion in concrete using cellular automaton, *J. Mater. Civ. Eng.*, **24** (2012), 783–788. https://doi.org/10.1061/(ASCE)MT.1943-5533.0000440

41. F. Biondini, A. Palermo, G. Toniolo, Seismic performance of concrete structures exposed to corrosion: case studies of low-rise precast buildings, *Struct. Infrastruct. Eng.*, **7** (2011), 109–119. https://doi.org/10.1080/15732471003588437
42. A. Titi, F. Biondini, Probabilistic seismic assessment of multistory precast concrete frames exposed to corrosion, *Bull Earthquake Eng.*, **12** (2014), 2665–2681. https://doi.org/10.1007/s10518-014-9620-2
43. F. Biondini, E. Camnasio, A. Palermo, Lifetime seismic performance of concrete bridges exposed to corrosion. *Struct. Infrastruct. Eng.*, **10** (2014), 880–900. https://doi.org/10.1080/15732479.2012.761248
44. A. Titi, F. Biondini, On the accuracy of diffusion models for life-cycle assessment of concrete structures, *Struct. Infrastruct. Eng.*, **12** (2015), 1202–1215. https://doi.org/10.1080/15732479.2015.1099110
45. X. Ruan, Y. Li, X. Y. Zhou, Z. R. Jin, Z. Y. Yin, Simulation method of concrete chloride ingress with mesoscopic cellular automata, *Constr. Build. Mater.*, **249** (2020), 118778. https://doi.org/10.1016/j.conbuildmat.2020.118778
46. J. J. Ma, P. Z. Lin, Simulation approach for random diffusion of chloride in concrete under sustained load with cellular automata, *Materials*, **15** (2022), 4384. https://doi.org/10.3390/ma15134384
47. M. L. Berndt, Properties of sustainable concrete containing fly ash, slag and recycled concrete aggregate, *Constr. Build. Mater.*, **23** (2009), 2606–2613. https://doi.org/10.1016/j.conbuildmat.2009.02.011
48. Ministry of housing and urban-rural development of the People's Republic of China, *Standard for Test Methods of Long-term Performance and Durability of Ordinary Concrete*, China Architecture & Building Press, Beijing, 2009.
49. F. Biondini, A. Nero, Cellular finite beam element for nonlinear analysis of concrete structures under fire, *J. Struct. Eng.*, **137** (2011). https://doi.org/10.1061/(ASCE)ST.1943-541X.0000307
50. J. Podroužek, B. Teplý, Modelling of chloride transport inconcrete by cellular automata, *Eng. Mech.*, **15** (2008), 213–222.
51. Q. Fu, Z. R. Zhang, Z. H. Wang, J. Q. He, D. T. Niu, Erosion behavior of ions in lining concrete incorporating fly ash and silica fume under the combined action of load and flowing groundwater containing composite salt, *Case Stud. Constr. Mater.*, **17** (2022), e01659. https://doi.org/10.1016/j.cscm.2022.e01659
52. F. Liu, Z. P. You, Z. P. A. Diab, Z. Z. Liu, C. Zhang, S. C. Guo, External sulfate attack on concrete under combined effects of flexural fatigue loading and drying-wetting cycles, *Constr. Build. Mater.*, **249** (2020), 118224. https://doi.org/10.1016/j.conbuildmat.2020.118224

AIMS Press